Annealing properties of the 0.5-ML Pd/Cu(100) surface alloy

G. W. Anderson and T. D. Pope
Interface Science Western and Department of Chemistry, University of Western Ontario, London, Ontario, Canada N6A 5B7

Kjeld O. Jensen*
Positron Beam Laboratory and Department of Physics, University of Western Ontario, London, Ontario, Canada N6A 5B7

K. Griffiths and P. R. Norton
Interface Science Western and Department of Chemistry, University of Western Ontario, London, Ontario, Canada N6A 5B7

Peter J. Schultz
Positron Beam Laboratory and Department of Physics, University of Western Ontario, London, Ontario, Canada N6A 5B7
(Received 12 March 1993; revised manuscript received 29 June 1993)

The annealing properties of the 0.5-monolayer Pd/Cu(100) surface alloy at 353 K have been investigated using reemitted-positron spectroscopy, low-energy electron diffraction, Auger electron spectroscopy, electron work function, and thermal-desorption spectroscopy. During the thermal treatment, Pd dissolution into the substrate is observed, with a time constant of ~33 min. In addition, near-surface defects (possibly steps) are observed to anneal out with a time constant of 82 min.

I. INTRODUCTION

The growth mechanisms and physical properties of epitaxial metal overlayers have been the focus of a great deal of experimental and theoretical research. Of particular interest is the ability to produce metastable structural phases, which are unstable in bulk material, by epitaxy onto a suitable substrate. These structural phases can often result in the creation of unique chemical[1] and electromagnetic[2] properties. Such systems are of both fundamental and practical interest, as they provide a way to investigate the interrelations between the growth, structure, and properties of materials. As the understanding of these relationships improves, it may become possible to engineer metallic heterosystems with specific properties by the choice of the appropriate materials and growth conditions.

The application of positron techniques to the study of metal overlayer systems has been developed recently.[3-7] The work function of an electron (ϕ^-) and positron (ϕ^+) in a metal can be defined according to

$$\begin{aligned} \phi^- &= D - \mu^- , \\ \phi^+ &= -D - \mu^+ , \end{aligned} \tag{1}$$

where D represents the surface dipole contribution and μ^- and μ^+ are the electron and positron chemical potentials (internal energies), respectively. The difference in charge between the electron and positron is responsible for the difference in sign of the dipole contribution, and leads to the possibility of a metal possessing a negative positron work function. In such a situation the total energy of the system is lower, with the positron just outside of the metal surface.

If low-energy (keV) positrons are implanted into a metal they rapidly thermalize and begin to diffuse freely through the sample. If a diffusing positron encounters the surface of a metal which has a negative work function then it may follow one of three branches: spontaneous reemission, localization into a surface state, or positronium formation through the pickup of a near-surface electron. Positrons may be reemitted either elastically, with energy equal to $-\phi^+$, or inelastically due to surface scattering. In reemitted-positron spectroscopy (RPS) the reemitted positrons are analyzed to provide information about the reemitting surface.

By measuring the RPS spectra as an overlayer is deposited onto a substrate, changes in the positron work function and surface scattering can be monitored. However, perhaps the greatest advantage of this technique stems from the sensitivity of positrons to various types of defects. Positrons are known to trap at open volume-type defects with great efficiency,[7] and surface defects have been shown to influence the positron surface branching ratios.[8] This results in RPS being one of a few techniques [others include scanning tunneling microscopy (STM), low-energy electron diffraction (LEED), and helium-atom scattering) capable of studying the evolution of defects in metal overlayer systems. This area of investigation has not yet fully matured, and interpretation of the results is still difficult. Nevertheless it posseses great potential due to its ability to measure a wide range of defects, both at and below the surface layer, over a large area.

Many studies of the growth of Pd overlayers on Cu(100) (Refs. 9-14) have focused primarily on the first 0.5 ML (monolayer) of deposition at 300 K. These studies have shown that the first 0.5 ML of Pd forms a well-ordered 50/50 Pd/Cu surface alloy with $c(2\times2)$ symmetry. In our laboratory RPS, low-energy electron diffraction (LEED), Auger electron spectroscopy (AES), electron work function, and thermal-desorption measurements have been utilized to investigate the growth and

morphology of Pd/Cu(100) overlayers from 0 to 37 ML thick. A preliminary report of RPS studies of the influence of defects in the thin-film Pd/Cu(100) system was published in Ref. 14, and in a subsequent publication we will discuss the properties of the thick Pd films. The present paper deals with the annealing properties of the 0.5-ML surface alloy deposited at 300 K.

II. EXPERIMENT

Three separate UHV chambers, (base pressure $< 1 \times 10^{-10}$ torr) each equipped with a Pd evaporation source, were utilized in this investigation. One of the chambers is equipped with a four-grid retarding field analyzer (RFA) for LEED and Auger experiments. It is interfaced to a variable energy, magnetically guided positron beam (described elsewhere[15]) for the positron reemission experiments. All of the positron measurements were performed using a 3-keV positron beam. This implantation energy ensured that most of the positrons thermalized in the sample prior to being reemitted.[16,17] The reemitted positrons are guided back along the beam axis and then deflected with $E \times B$ plates to a channel electron multiplier detector, where they are counted (see Fig. 1). Energy analysis of the positrons is accomplished by applying a retarding bias to a 90% transmission grid. A Ge detector was also utilized to detect the γ rays produced by positron-electron annihilations in the sample.

The second chamber is equipped with a similar RFA for LEED and AES, a Kelvin probe for electron work-function measurements, and a collimated quadrupole mass spectrometer for thermal-desorption spectroscopy (TDS) measurements. The LEED images were collected by a silicon-intensified (SIT) video camera from the LEED screen and stored on video tape. The VCR is interfaced to a computer through a frame grabber board, allowing subsequent measurement of the LEED spot intensities and full widths at half maximum (FWHM's). The third UHV chamber is equipped with a cylindrical mirror analyzer (CMA) for high-resolution AES measurements. The CMA is interfaced to a computer, allowing the monitoring of AES peak amplitudes with time.

The Cu(100) substrates were cut from a single-crystal Cu boule and aligned to within $\pm 0.5°$ by Laue x-ray measurements. The samples were polished using various grades of diamond paste and finally a 0.05-μm alumina slurry. The samples were cleaned by Ar^+-ion bombardment (1–2 keV, 1 $\mu A\,cm^{-2}$) at room temperature and subsequently annealed at 700 K. Surface cleanliness was confirmed by AES measurements. The Pd overlayers were deposited from a sublimation source onto a Cu(100) substrate at 295 K. The Pd coverage (accurate to ± 0.05 ML) was determined from previously established AES and LEED calibrations.[13]

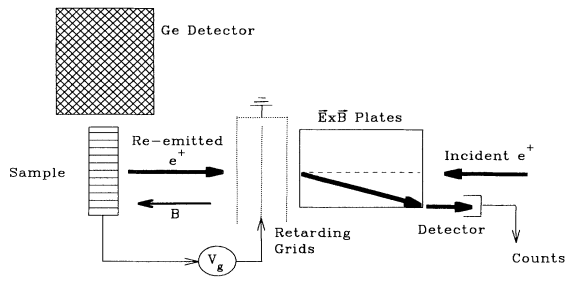

FIG. 1. A schematic representation of the experimental setup for the positron measurements.

III. RESULTS

The annealing behavior of 0.5-ML Pd overlayers on Cu(100) was investigated by RPS, LEED, AES, electron work function, and TDS measurements. In all experiments the samples were prepared at 295 K and then ramped to the annealing temperature of 353 K at a heating rate of approximately 1 K/s.

RPS was utilized to look at the positron work function, scattered fraction, and reemission yield as functions of anneal time. Figure 2 displays the integral and differentiated RPS spectra for 0.5-ML Pd/Cu(100) overlayer. The peak in the differential spectrum, which represents the elastically reemitted positrons, occurs at an energy given by $E_3 = \phi^+ + \phi^- - \phi_g^-$, where ϕ_g^- is the work function of the analyzing grids.[6] During reemission some of the positrons are scattered, resulting in a low-energy tail extending from the elastic reemission energy down to zero kinetic energy. This point of zero kinetic energy, given by $E_1 = \phi^- - \phi_g^-$, represents the zero of

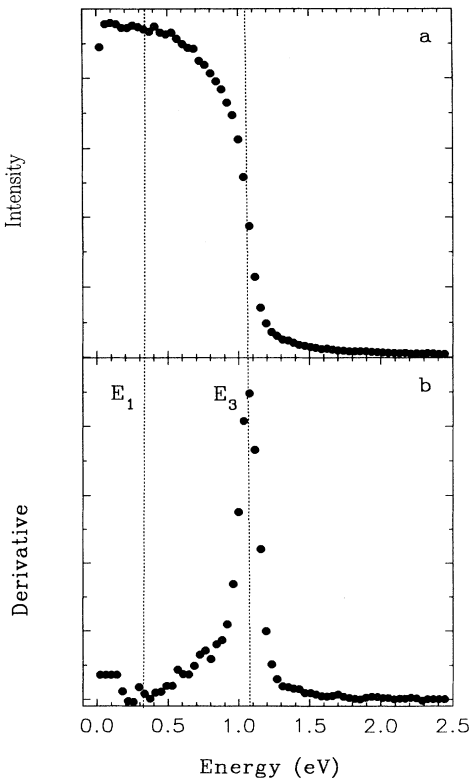

FIG. 2. The RPS spectra (taken with the sample normal parallel to the incident beam direction) and its derivative for a 0.5-ML Pd/Cu(100) sample, showing the elastic peak (E_3) and the energy cutoff (E_1).

kinetic energy for the system, which is defined as the contact potential difference between the sample and the analyzing grids. The positron work function can therefore be determined according to $\phi^+ = E_3 - E_1$.

By examining the detailed energetics of the RPS spectra, information about the source of work-function changes can be obtained. If, in the course of an experiment E_1 is observed to change while E_3 remains constant, then $-\Delta\phi^+ = \Delta E_1 = \Delta\phi^-$, assuming that the work function of the grids remains constant. Combining this with Eq. (1) yields the result that in this situation the change in work function is due to a change in the surface dipole only. E_3 will be observed to change only if there is a change in the sum of the electron and positron chemical potentials.

The positron work function was found to be unaffected (within the range of experimental error) by annealing for up to 5 h. The sensitivity of the measurement was such that any change of work function greater than 40 mV could be detected. However, when the RPS spectra are examined, both the E_1 and E_3 peaks are found to shift to lower energy by 60 mV. As previously explained, the shift in E_3 requires that the sum of the positron and electron chemical potentials is changing, which suggests that the bulk substrate is being altered in some manner. In this situation the electron and positron work-function changes are not solely due to a surface dipole effect, and thus would not be expected to be related in any simple manner.

The fraction of positrons which are scattered during reemission is determined by comparing the relative areas of the elastic peak (fit with a Gaussian) and the low-energy tail in the differential RPS spectrum. The fraction of positrons in this tail arises both from inelastic and elastic scattering, since any elastic-scattering event which leads to off-normal positron emission will result in a lower observed positron energy.[3,6,7,14,18] The scattered fraction of reemitted positrons was monitored before and after annealing for two different times. In one experiment the scattered fraction remained constant over a 50-min anneal. However, in the second case the scattered fraction was observed to decrease from 0.33 ± 0.03 to 0.26 ± 0.02 during a 5.5-h anneal. This observation is attributed to the removal of defects capable of scattering positrons.

The effect of the annealing treatment on the positron-reemission yield is illustrated in Fig. 3. Y^+ was measured before the start of the anneal and as a function of time for both clean Cu(100) and 0.5-ML Pd/Cu(100) samples. In all experiments there is an initial drop in Y^+ immediately upon the start of annealing, with an equivalent increase in Y^+ observed upon cooling the samples. This initial drop is attributed to a reversible temperature effect associated either with the positron diffusion constant or the positron surface branching ratios.

In the case of the clean Cu(100) sample, after the initial drop, Y^+ is observed to remain constant over a 120-min anneal, indicating that the thermal treatment is having no effect on the surface. However, in the case of the 0.5-ML Pd/Cu(100) samples Y^+ is observed to increase, in a manner well described by $Y^+(t) \propto [1 - \exp(-t/\tau)]$, ulti-

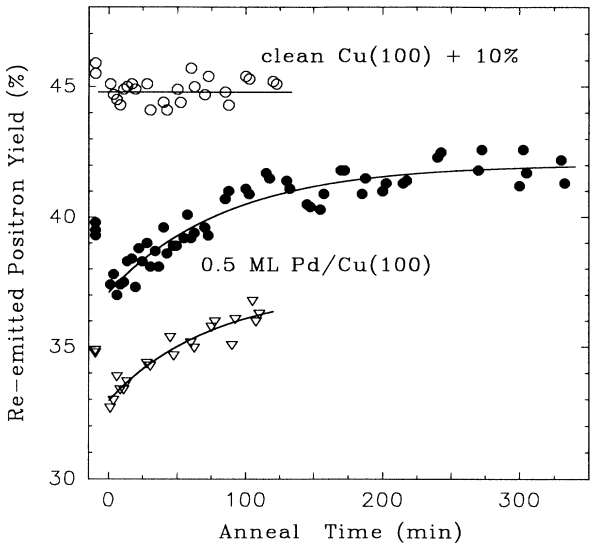

FIG. 3. Reemitted-positron yield as a function of annealing time at 353 K for clean Cu(100) (offset by +10% for display purposes) and two 0.5-ML Pd/Cu(100) samples.

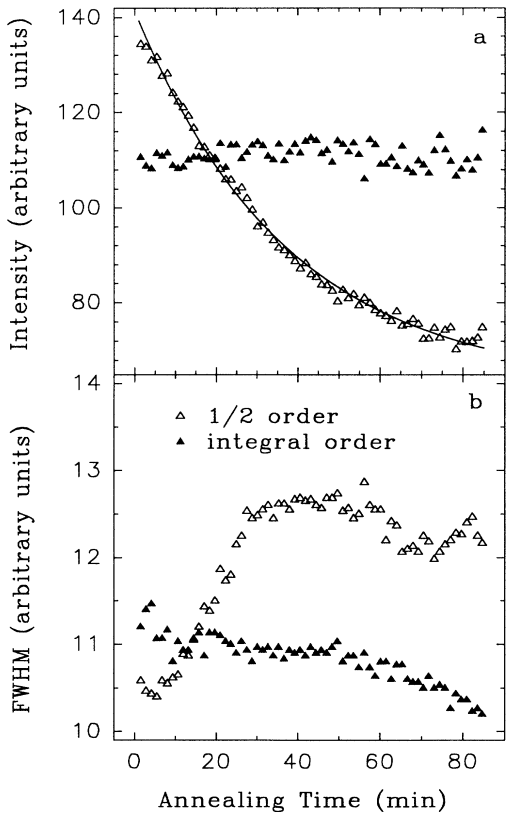

FIG. 4. (a) The intensity and (b) FWHM of the (1,1) integral (filled triangles) and half-order (open triangles) LEED spots for 0.5-ML Pd/Cu(100) as a function of annealing time at 353 K.

mately improving by ~5% over a 6-h anneal. Since the positron work function, which is known to correlate with Y^+ (Refs. 14 and 19) has been observed to remain constant during the anneal, this increase cannot be associated with positron work-function changes. By fitting the data a time constant of $\tau=82\pm5$ min is obtained. It is proposed that this phenomenon is related to the annealing out of defects in the system.

Figure 4 displays the dependence of the intensity and FWHM of the integral and half-order LEED spots on annealing time. The (1,0) integral-order spots, which correspond to the Cu(100) substrate and the alloy layer (most of the intensity is from the substrate at the 125-eV electron energy used), are observed to sharpen slightly while remaining constant in intensity during the anneal. The half-order spots, due to the surface alloy, decrease in intensity by about 50% during the anneal. This decrease in intensity has been fit with a function of the form $I \propto e^{-t/\tau}+I_0$, yielding a time constant of $\tau=37\pm1$ min (see the solid line in Fig. 4). The FWHM of the half-order spots is observed to increase to a plateau region and finally decrease slightly after about 60 min of annealing.

The broadening of the half-order spots is due to the loss of long-range order in the alloy during the anneal. This is interpreted as evidence of a loss of some Pd from the surface alloy and its replacement with Cu, resulting in a less ordered alloy surface or smaller alloy islands. The slight sharpening of the spots after 60 min may be due to subsequent ordering of the remaining alloy, the coalescence of alloy islands, and/or the ordering of some of the Pd in a subsurface layer. The loss of Pd from the surface would also produce the decrease in spot intensity. This result is consistent with that observed for the integral order spots, as the slight decrease in the integral order spot width is indicative of improvement in the long-range order of the Cu atoms during the anneal.

While it is not possible to determine what is happening to the Pd from these data, two possibilities are dissolution into the bulk and the formation of an ordered underlayer. Formation of such an ordered underlayer has been suggested following annealing of the (110) surface of the Cu_3 Pd bulk alloy.[20] This issue was examined further using AES, electron work function, and TDS experiments.

To verify the interpretation that Pd is being lost from the surface, the Pd and Cu AES signals were monitored during annealing (see Fig. 5). The 60-eV Cu Auger transition was monitored and showed an initial increase over the first 20 min of annealing, and then remained constant. This is consistent with the removal of some Pd from the surface, and its subsequent replacement by Cu atoms. However, the Pd (330+326 eV) Auger signal remained relatively constant over this same initial time range, being observed only to decrease (in an exponential fashion) after annealing for 20 min. After 100 min of annealing the Pd AES signal was observed to have decreased by 10%. This may indicate that for this first part of the anneal, while some Pd is migrating away from the surface, it has not been moved far enough to significantly affect its AES signal (escape depth ~10 Å). The magnitude of the increase of the Cu signal during this phase must be related to the greater surface sensitivity due to the much lower characteristic Auger electron energy (escape depth ~5 Å). As the anneal continues, the Pd is removed far enough from the surface that its AES signal is observed to decrease. The data, for the region where the Pd signal is decreasing, have again been fit with a function of the form $I \propto e^{-t/\tau}+I_0$, and gives a time constant of 33 ± 5 min, in good agreement with the LEED results.

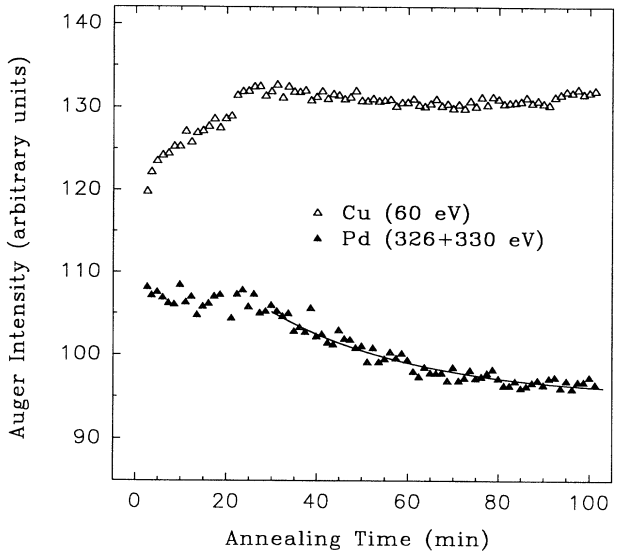

FIG. 5. The Pd (326+330 eV) and Cu (60 eV) Auger-transition-integrated intensities of 0.5-ML Pd/Cu(100) as a function of annealing time at 353 K. The solid line represents the fit to the data as discussed in the text.

The annealing of 0.5ML Pd/Cu(100) overlayers at 353 K was also studied by electron work-function measurements, as shown in Fig. 6. The work-function values

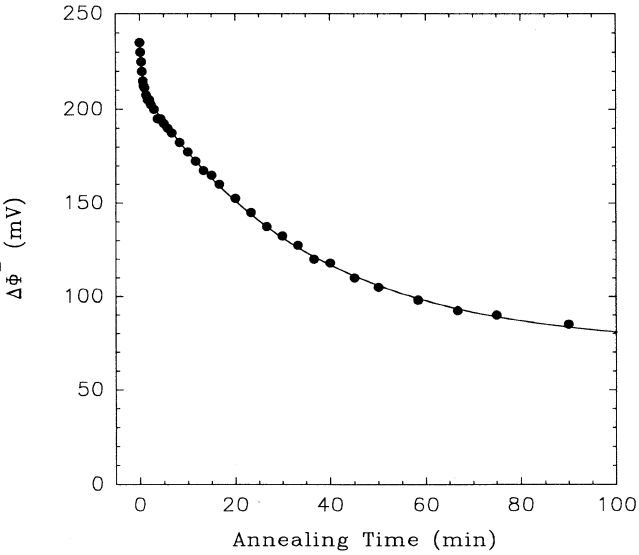

FIG. 6. The change in the electron work function of 0.5-ML Pd/Cu(100) during annealing at 353 K. The work-function values shown are referenced to that of the clean Cu(100) sample.

presented are relative to that of clean Cu(100). The electron work function is observed to decrease rapidly over the first minute of the anneal, followed by a slower exponential decrease with a time constant of $\tau=34.4\pm0.9$ min. These results are consistent with the removal of some Pd from the surface during the anneal, which would be expected to lower the work function, and the time constant is consistent with both the LEED and AES results.

TDS measurements were utilized to look at the surface composition at different stages of annealing. CO was adsorbed onto the surface at ~ 100 K to saturation, and the desorption was monitored with the collimated mass spectrometer as the sample was heated. Figure 7(a) displays the TDS spectra as a function of the anneal time. The two lower-temperature desorption features are identified as being due to desorption from Cu sites, while the high-temperature feature is due to desorption from Pd sites.[21]

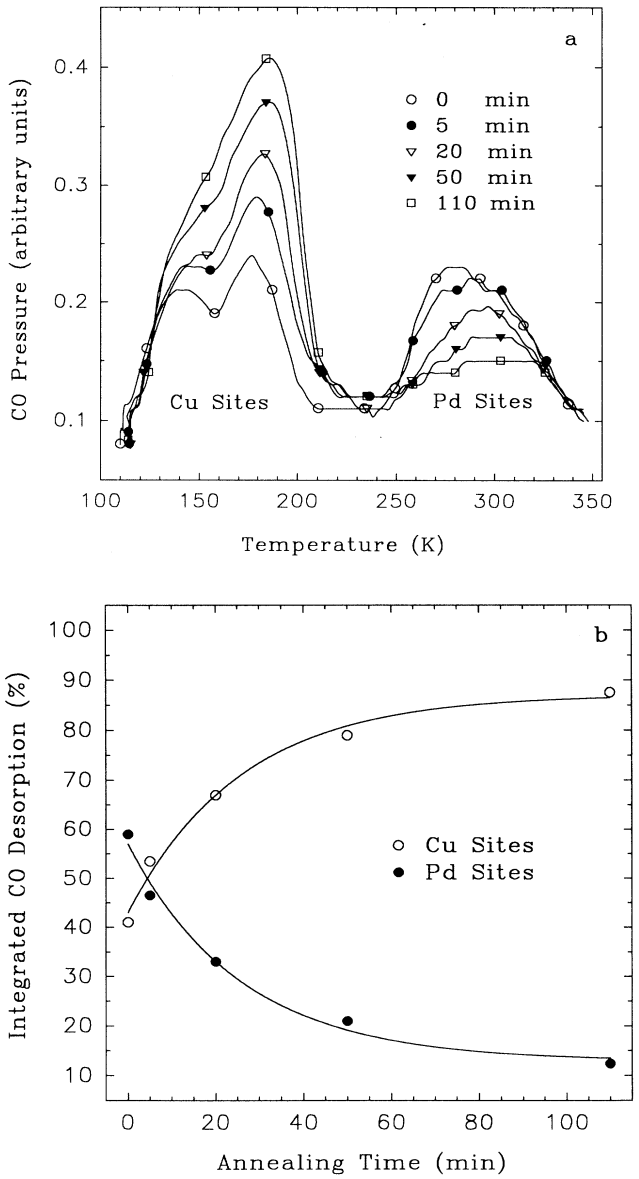

FIG. 7. (a) TDS spectra of CO on 0.5-ML Pd/Cu(100) which had been annealed for different times at 353 K. (b) The relative integrated amounts of CO desorbed from Cu and Pd sites as a function of annealing time at 353 K.

The CO is known to be bound to on-top sites on Pd and Cu in the $c(2\times2)$ alloy structure,[21] and therefore the amount of CO desorbed from each species is related to its surface coverage. Figure 7(b) displays the relative integrated areas of both the Cu- and Pd-related CO desorption features as a function of anneal time at 353 K. Initially 59% of the desorbed CO comes from Pd sites. There is evidence to suggest that the Cu-like binding sites have not been saturated, since desorption from these sites is observed to begin immediately with heating. This could explain the higher than expected fraction of Pd-site desorption. This fraction is observed to decrease with annealing in an exponential manner, with a time constant of $\tau=26\pm6$ min. This decrease shows that Pd is being removed from the surface during the anneal, and is being replaced by Cu. After a 110-min anneal only 12.4% of the CO desorbs from Pd sites, a 79% decrease from the initial value.

IV. DISCUSSION

The annealing properties of 0.5-ML Pd/Cu(100) (deposited at 295 K) at 353 K were investigated by a variety of techniques. AES, electron work function, and TDS measurements all indicate that Pd is being removed from the surface during the anneal. In the TDS measurements of CO desorption, which are the most surface sensitive, it was observed that during a 110-min anneal a significant number ($>70\%$) of Pd-like binding sites are removed from the surface. At the same time the LEED intensity of the half-order spots is observed to decrease by approximately 50%. The AES observations for the first 20 min of annealing support a place exchange model between the surface and second layer, a suggestion which is consistent with the LEED observations.

It is proposed that during the initial stage of the anneal some of the Pd migrates from the surface alloy to a second layer which may be partially composed of an ordered alloy, and the surface-layer Pd is replaced by Cu. As the anneal continues some of the Pd from the second layer diffuses further from the surface and is replaced by additional Pd from the surface. This interpretation is consistent with the positron work-function measurements, which show that a bulk property (the sum of the positron and electron chemical potentials) is changing during the anneal. The Pd which migrates away from the second layer does not migrate far, as the AES signal is only observed to decrease by 10% (the escape depth for 330-eV Pd Auger electrons is ~ 10 Å). A time constant of ~ 33 min has been observed for the overall process of Pd dissolution by LEED, AES, TDS, and electron work-function measurements.

The measurements of the positron yield and scattered fraction suggest that defects are being annealed out of the sample during the thermal treatment. This process occurs with a time constant of 82 ± 5 min, which is a slower time scale than the Pd migration away from the

surface. It is possible that the defects were (i) originally present in the near-surface region of the Cu(100) substrate, (ii) associated with surface damage of the substrate, or (iii) introduced in the Pd film during deposition. In all three cases we suggest that the observed annealing was assisted by Pd diffusion, both along the surface of the overlayer and into the substrate, and the accompanying diffusion of Cu atoms. The ($\sim 2\times$) longer time constant for defect recovery indicates that the process is diffusion limited, due to the necessity of interaction between two dilute distributions of (mobile) Pd atoms and (static) defects.

Of the three possibilities listed above, we favor the third model of defects grown into the film itself. Our "starting" yields of $Y^+ \sim 35-40\,\%$ for clean Cu(100) are as high as any observed for clean, well-annealed Cu,[6,20] indicating that no significant concentration of positron-trapping defects are present. In addition, no effect was observed in the positron yield measurements of the annealing of the Cu substrate. It is not possible to determine what these defects are, but one possibility is steps associated with macroscopic terraces which affect the positron surface branching ratios. Large terraces ($> \sim 100$ Å) would not be detected by the other techniques and would require that a large amount of Pd be moved to reduce the defect concentration.

The combination of experimental techniques employed in the present study underscores the need for a broad spectrum of information if one is to untangle complex issues associated with the growth and dynamics of interesting and potentially practical heterostructures. In the present study several surface-sensitive techniques, including TDS, AES, LEED, electron work function, and RPS were combined. Data are considered in relation to the specific depth and structural sensitivities of each of these techniques, which allows us to develop the microscopic model for the growth and annealing of Pd on Cu(100) contained in the present and previous[13,14] discussions.

ACKNOWLEDGMENTS

This work was partially funded by the Natural Sciences and Engineering Research Council of Canada and the Network of Centres of Excellence in Molecular and Interfacial Dynamics (CEMAID), supported by the Government of Canada.

*Present address: System Research Division, British Telecom Laboratories, Martlesham Heath, Ipswitch 1P5 7RE, U.K.

[1]C. T. Campbell, Ann. Rev. Phys. Chem. **41**, 775 (1990).
[2]S. D. Bader, J. Magn. Magn. Mater. **100**, 440 (1991); A. J. Freeman and R. Wu, *ibid.* **104-107**, 1 (1992).
[3]P. J. Schultz, K. G. Lynn, W. E. Frieze, and A. Vehanen, Phys. Rev. B **27**, 6626 (1983).
[4]D. W. Gidley and W. E. Frieze, Phys. Rev. Lett. **60**, 1193 (1988).
[5]D. W. Gidley, Phys. Rev. Lett. **62**, 811 (1989).
[6]J. G. Ociepa, P. J. Schultz, K. Griffiths, and P. R. Norton, Surf. Sci. **225**, 281 (1990).
[7]P. J. Schultz and K. G. Lynn, Rev. Mod. Phys. **60**, 701 (1988).
[8]A. R. Köymen, D. W. Gidley, and T. W. Capehart, Phys. Rev. B **35**, 1034 (1987).
[9]G. W. Graham, Surf. Sci. **171**, L432 (1986).
[10]S. H. Lu, Z. Q. Wang, S. C. Wu, C. K. C. Lok, J. Quinn, Y. S. Li, D. Tian, F. Jona, and P. M. Marcus, Phys. Rev. B **37**, 4296 (1988).
[11]S. C. Wu, S. H. Lu, Z. Q. Wang, C. K. C. Lok, J. Quinn, Y. S. Li, D. Tian, F. Jona, and P. M. Marcus, Phys. Rev. B **38**, 5363 (1988).
[12]G. W. Graham, P. J. Schmitz, and P. A. Thiel, Phys. Rev. B **41**, 3353 (1990).
[13]T. D. Pope, G. W. Anderson, K. Griffiths, P. R. Norton, and G. W. Graham, Phys. Rev. B **44**, 11 518 (1991).
[14]G. W. Anderson, K. O. Jensen, T. D. Pope, K. Griffiths, P. R. Norton, and P. J. Schultz, Phys. Rev. B **46**, 12 880 (1992).
[15]P. J. Schultz, Nucl. Instrum. Methods B **30**, 94 (1988).
[16]B. Nielsen, K. G. Lynn, and Y. C. Chen, Phys. Rev. Lett. **57**, 1789 (1986).
[17]H. Huomo, A. Vehanen, M. D. Bentzon, and P. Hautojärvi, Phys. Rev. B **35**, 8252 (1987).
[18]C. A. Murray and A. P. Mills, Jr., Solid State Commun. **34**, 789 (1980).
[19]E. M. Gullikson, A. P. Mills, Jr., and C. A. Murray, Phys. Rev. B **38**, 1705 (1988).
[20]D. J. Holmes, D. A. King, and C. J. Barnes, Surf. Sci. **227**, 179 (1990).
[21]S. H. Lu, J. Yao, L. Zhu, G. L. Liu, F. Q. Liu, and S. C. Wu, Phys. Rev. B **45**, 6142 (1992).